A Novel Interference Safety Margin for Cognitive Radio MANET using Smart Antennas

Mathieu Boutin
INRS-EMT (University of Quebec), Montreal, Canada
LRTCS-UQAT, Val d'Or, Canada
Email: mathieu.boutin@emt.inrs.ca

Charles Despins[1,2,3], Tayeb Denidni[1,2] and Sofiène Affes[1,2]
1: INRS-EMT (University of Quebec), Montreal, Canada
2: LRTCS-UQAT, Val d'Or, Canada
3: PROMPT Inc., Montreal, Canada
Emails: cdespins@promptinc.org, tayeb.denidni@emt.inrs.ca, affes@emt.inrs.ca

***Abstract*—A new interference estimation technique is proposed for the deployment of a smart-antenna-equipped MANET (Mobile Ad hoc NETwork), acting as a secondary network, sharing the same scarce frequency band as many legacy fixed antennas (primary network) in the same area. With the help of only a coarse probabilistic estimate of each primary antenna location, the MANET can voluntarily overestimate the aggregate interference it causes to the primary network. The latter indeed imposes an aggregate interference safety margin for the former to respect, following a chosen minimum probability. By means of simulations prior to deployment, the MANET can thus assess the impact of its future spectrum sharing with the primary network, and take countermeasures accordingly. The proposed technique offers great potential, for the deployment of a cognitive MANET, since advances in millimeter radio waves technologies will soon make smart antennas easily portable in size.**[1]

***Index Terms*—cognitive radio, interference estimation, interference safety margin, mobile ad hoc network, probabilistic location, smart antennas, uncertainty circle.**

I. INTRODUCTION

Significant challenges must be faced when a wireless network of any kind spatially and spectrally shares the same environment of an already well-established legacy wireless network. Research progress on spectrum sharing strategies is therefore highly sought as, according to many radio spectrum measurement results reported as in [1-2], a large proportion of the licensed spectrum remains mostly unused or under-utilized. This indicates that the current spectral shortage may be partially relieved by a more flexible user access rather than the presently rigid and static spectral allocation [3].

The relatively new and promising cognitive radio concept allows a wireless network to be spectrally aware of its surroundings and to further take intelligent decisions accordingly. For instance, packets routing, power control, medium access control or link scheduling highly depend on the sensed spectral availability so as to minimize the interference. In the context of an unlicensed (secondary) wireless network deployed in the same area as a fixed legacy and licensed (primary) wireless network, using the same frequency band, the sensing function is one of the most important attributes of cognitive radios – as it ensures non-interference to licensed users – and should involve more sophisticated techniques than simple determination of power in a frequency band [4].

Based on the fact that a secondary and a primary network would usually interact the least possible with each other, if the former is to be qualified as "non-intrusive" [3] then the primary network would not adapt its activities because of the secondary network's presence, but rather the opposite shall occur. The scheme we propose is to let the primary network impose an interference protection requirement to be respected by the secondary network, such that the latter can assess if its (ad-hoc) deployment is acceptable. The main obstacle lies in the secondary network's knowledge of the location of each fixed primary antenna. In fact, the very poor interaction between both networks only allows the secondary network to have a probabilistic estimate of those antennas, possibly with a serious lack of accuracy. The primary network managers being aware of this problem, the interference protection requirement is thus supplemented with a minimum probability of being respected. A new interference estimation technique is therefore proposed for the secondary network to voluntarily overestimate the interference it causes to the primary network, so an interference safety margin can be respected with respect to the estimate, following the aforementioned minimum probability.

[1] This work was presented in part at the ICWCUCA'08, Val d'Or, Canada, August 25-27, 2008. Manuscript received November 30, 2008; revised March 13, 2009; accepted April 15, 2009.

Our scheme could be applied to more conventional structured networks such as cellular networks, as well as to ad hoc networks such as sensors networks or MANET (mobile ad hoc network). In this paper, we however focus our work on MANET deployments. Considering a structure-free wireless network is highly relevant as this kind of network is attractive for a very large scope of applications such as military interventions, emergency rescues, short-term mine gallery exploitation and any other type of mission critical, temporary, fast and low cost wireless communication deployment.

This paper also emphasizes the use of smart antennas by the MANET. Smart antenna transceivers currently have an adequate size and weight to equip vehicles. However, with advances in millimeter-wave radio technologies, such a transceiver could be worn by a single person in the very near future. By using a smart antenna, a network node is not restricted to transmit and receive with an omnidirectional radiation pattern antenna. Instead, by means of multiple antennas at the transceiver, forming an antenna array, a node can smartly choose the direction and width of its radiation beam by properly tuning its transceiver tap weight coefficients. This transmission and reception directivity may also be exploited to allow different networks to coexist in close proximity even if they share the same frequency band, since spectrum is a very scarce resource [4]. Nonetheless, we do not delve into the details of beam steering or beam width adaptation of such antennas, as we rather consider a very useful and inspiring application.

The main problem description is first presented and supported by a review of related research, followed by our system models, the detailed explanation of our proposed interference estimation technique, and finally simulation results and interpretation before concluding.

II. Problem Description and Related Research

In [5], pilots allow secondary network users to measure the local SNR of the primary signal which is used to approximate the distance from a primary transmitter. In this way, secondary users can adjust their transmission power accordingly to avoid interfering with primary antennas. However, since this gives too little information about the primaries, secondary users must be quiet within a "no-talk radius". Not only is the secondary network penalized in this scheme by using omnidirectional antennas, but also for never estimating the aggregate interference it causes to the primary network.

The proposed idea in [3] is that a transmitting secondary node equipped with a smart antenna can construct its transmission beam pattern such that its interference to a receiving primary antenna is either minimized or constrained. Furthermore, combined with transmission power control, the aggregate interference at a primary antenna can be limited below a predefined power threshold. However, because of the constraint on its interference to the primary antenna, the secondary node cannot be arbitrarily deployed. The goal is then to determine the region where the secondary node can be deployed using smart antennas.

To the best of our knowledge, in the research field of cognitive radios and spectrum sharing, no such technique for allowing a smart-antenna-equipped secondary network to probabilistically ensure an interference protection margin to a primary network has previously been proposed yet. Indeed, our approach is almost entirely based on the knowledge of the secondary network about the imprecise probabilistic location of each fixed antennas of the primary network. Our contribution lies in a new proposal for such a spectrum sharing condition imposed by the primary network on the secondary network, so that interference assessments prior to the secondary network deployment could allow both primary and secondary networks to assess the impact of the secondary network's real world operation, and to take countermeasures accordingly.

The next subsections introduce the issues brought by the knowledge of only the probabilistic locations of primary antennas by the MANET, as well as the aggregate interference safety margin requirement from the primary network, which is the core of our contribution. In the remainder of this paper, the set of all primary antennas is defined as S_P, and the set of all transmitting and receiving nodes are defined as S_T and S_R, respectively. We only consider the interference caused by the MANET to the primary antennas, which are assumed to be constantly in receiving mode for a worst case assessment.

A. Probabilistic location of primary antennas

In this work, we assume the MANET to be unaware of the exact location of each primary antenna, upon its deployment in the same area as the primary network, but to rather have a coarse estimate. Several techniques have been proposed over the years for sensor networks and MANET to estimate the location of primary transceivers. In [6], it has been shown that it is possible to take advantage of the local oscillator leakage power emitted by all passive primary network devices to detect their location for cognitive radios. Location uncertainty of primary devices is addressed in [7] as a function of cognitive radio receiver density. In [8-9], multiple transmitter localization is performed by particle swarm optimization and expectation maximization techniques, with a precision highly dependent on the number of cognitive receiving nodes, number of primary transmitters, radio propagation model assumptions, and the spatial clustering as initial conditions for the iterative algorithms.

Location estimates, such as the expectation, are much more useful if they are complemented with some indication about their precision [10]. In order to visualize the uncertainty associated with the location of each primary antenna, we assume that we have a probability distribution describing the uncertainty about the actual location. This can be done by drawing an ellipse centered at the expected location such that the orientation and size of the ellipse describes the uncertainty of the location estimate as well as possible [10].

We thus assume that the MANET location estimate of each primary antenna p is modeled as a bivariate

Gaussian random variable with means $\mu_x(p)$ on the abscissa and $\mu_y(p)$ on the ordinate, and standard deviation $\sigma_{xy}(p)$ on both axes for simplicity. We thus obtain an uncertainty circle (UC) with radius $R_{UC}(p) = \Omega_{UC}\sigma_{xy}(p)$, where Ω_{UC} is the uncertainty coefficient, for each primary p and centered at $(\mu_x(p),\mu_y(p))$. Considering an uncertainty ellipse instead of an uncertainty circle would be more realistic and is left for our future work. The actual location of each primary p is defined as $(x(p),y(p))$, but is unknown by the MANET.

The choice of Ω_{UC} is of key importance when it comes for the MANET to prevent itself from highly interfering with the primary antennas, while still guarantying an acceptable QoS to its nodes.

B. The aggregate interference safety margin

A single node of the MANET may generate interference to one or many primary antennas while transmitting toward any other MANET node. We denote as $I_R(i,p)$ the interference received by a primary antenna p from a single transmitting node i. However, a primary antenna cannot distinguish between individually received interference from transmitting nodes, as it only perceives an aggregate interference denoted as $I_A(p)$, which is the sum of all individual interference from transmitting nodes at a given instant and defined as:

$$I_A(p) = \sum_{\forall h \in S_T} I_R(h,p). \quad (1)$$

Since we assume the MANET and primary network to not be able to communicate any information, the MANET unfortunately never knows $I_A(p)\ \forall p \in S_P$. Nonetheless, because the probabilistic location of each primary antenna is known by the MANET, as well as the exact location of each node and the radio propagation path loss exponent, the MANET can at least estimate $I_R(i,p)$ for a transmitting node i potentially interfering with a primary antenna p, and we denote this estimated interference as $I_{R,e}(i,p)$. Consequently, the MANET can also estimate $I_A(p)$, and we denote this estimated aggregate interference as $I_{A,e}(p)$, simply defined from (1) as:

$$I_{A,e}(p) = \sum_{\forall h \in S_T} I_{R,e}(h,p). \quad (2)$$

To better differentiate $I_R(i,p)$ from $I_{R,e}(i,p)$ and $I_A(p)$ from $I_{A,e}(p)$, we call $I_R(i,p)$ the "actual" received interference from i to p, and we call $I_A(p)$ the "actual" aggregate interference on p.

There is inevitably a difference or error between $I_{A,e}(p)$ and $I_A(p)$ for all $p \in S_P$, as it becomes impossible for the MANET to exactly predict all radio propagation phenomena from nodes to primary antennas such as slow and fast fading, reflection, refraction, diffraction and so on [11]. In our scheme, it is more appropriate to talk of an aggregate interference offset on p, denoted as $I_{A,o}(p)$, instead of an aggregate interference error, as this difference can be probabilistically selected by the MANET at the advantage of the primary network as explained subsequently. Thus, we define the aggregate interference offset on p as:

$$I_{A,o}(p) = I_{A,e}(p) - I_A(p). \quad (3)$$

If $I_{A,o}(p) \leq 0$, then the MANET has underestimated the interference it causes to p, and the future MANET decisions based on $I_{A,e}(p)$ are more likely to be harmful for p (we include $I_{A,o}(p) = 0$ as an underestimation for convenience only). On the other hand, if $I_{A,o}(p) > 0$, then the MANET has overestimated the interference it causes on p, and the future MANET decisions are less likely to be harmful for p, but more likely to decrease the MANET communication efficiency. Since the values of $I_{A,e}(p)\ \forall p \in S_P$ have great influence on future MANET decisions, which in turn have a direct impact on the interference caused to the primary network, the latter could accept to share it precious frequency band with the former only if some restriction applies to $I_{A,o}(p)\ \forall p \in S_P$.

In our scheme, we assume the primary network to impose an aggregate interference safety margin, denoted as $I_{A,SM}$, for the MANET to respect following a given safety margin probability denoted as η_{SM}, where $0 \leq \eta_{SM} \leq 1$. $I_{A,SM}$ and η_{SM} are assumed to be constant and the same for all primary antennas, for simplicity. However, using different values of $I_{A,SM}$ and η_{SM} for each antenna would be very easy to implement, as a generalization of our present work. The primary network thus accepts to share its spectrum with the MANET if and only if the following requirement is met by the latter:

$$P\left(I_{A,o}(p) > I_{A,SM}\right) \in [\eta_{SM}, 1], \forall p \in S_P. \quad (4)$$

It is then up to the MANET to assess if it can meet this requirement while still providing an acceptable QoS among its nodes.

III. System Models

We assume that each node of the MANET has only one half-duplex transceiver. The same frequency band is used by both the MANET and primary network. There is no possible communication between both networks. We omit temporal details about whether communication among nodes is synchronous (like TDMA) or asynchronous (like CSMA), and the protocols used, as those do not influence our simulations results. The following subsections present our propagation and antenna model, as well as our communication and interference model.

A. Propagation and antenna model

We use roughly the same antenna model as in [12]. Suppose we have a transmitting node i and receiving node j. Let $G_T(i) = 2\pi/\theta(i)$, where $G_T(i)$ is the antenna gain of the transmitting node i, with its beam width $\theta(i)$ and beam direction $\varphi(i)$. Similarly, let $G_R(j) = 2\pi/\theta(j)$, where $G_R(j)$ is the antenna gain of the receiving node j with its beam width $\theta(j)$ and beam direction $\varphi(j)$. Antenna beams are modeled as circle sectors, as we assume the main lobe to be much more important than all the side lobes together. For the remainder of this paper, we use the word "sector" instead of "circle sector".

Let $d(i,k)$ be the distance between i and any receiver k (node or primary antenna). The path loss gain $G_\alpha(i,k)$ with path loss exponent α of the transmitted power as a function of $d(i,k)$, by considering a constant unitary gain for a distance smaller than the reference distance d_0 , is defined by:

$$G_\alpha(i,k)=\begin{cases} C(i,k), & \forall d(i,k)\in[0,d_0] \\ d(i,k)^{-\alpha}\,C(i,k), & \text{otherwise} \end{cases}, \quad (5)$$

where $C(i,k)$ is a zero mean Lognormal random variable, with standard deviation σ_C, representing the slow fading on the radio channel between i and k, as in [11]. There is no need to consider the fast fading since we assume it to be averaged in our model.

Let $\psi(i,k)$ be the angle between positions $(x(i),y(i))$ and $(x(k),y(k))$ of node i and receiver k, respectively, and let $\psi(k,i)$ be the angle between $(x(k),y(k))$ and $(x(i),y(i))$. Also, let $\Delta_T(i,k) = |\varphi(i) - \psi(i,k)|$ and $\Delta_R(i,k) = |\varphi(k) - \psi(k,i)|$. Since $\psi(i,k)$, $\psi(k,i)$, $\varphi(i)$ and $\varphi(k)$ are angles indicating a direction, they must be relative to the same reference. We define a binary gain $G_{TR}(i,j)$, taking either the value 1 or 0, depending on whether the receiving node j can receive transmitted power from node i as per the width and direction of both antenna beams, by the following equation and shown on Fig. 1:

$$G_{TR}(i,j)=\left(\Delta_T(i,j)\le\frac{\theta(i)}{2}\right)\wedge\left(\Delta_R(i,j)\le\frac{\theta(j)}{2}\right). \quad (6)$$

The grey line shown on Fig. 1, joining nodes i and j, and passing through both sectors, represents the condition to obtain $G_{TR}(i,j) = 1$. If we let $P_T(i)$ be the transmission power of node i, and $P_R(i,j)$ be the received power at node j from i only, then we have:

$$P_R(i,j)=P_T(i)G_T(i)G_R(j)G_\alpha(i,j)G_{TR}(i,j). \quad (7)$$

We define a binary gain $G_{TP}(i,p)$, taking either the value 1 or 0, depending on whether node i can cause interference to the primary antenna p as per the width and direction of i's antenna beam, by assuming that all primary antennas are omnidirectional, with the following equation:

$$G_{TP}(i,p)=\begin{cases} 1, & \text{if } \Delta_T(i,p)<\theta(i)/2 \\ 0, & \text{otherwise} \end{cases}. \quad (8)$$

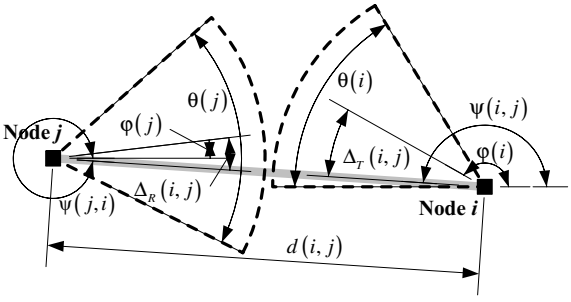

Figure 1. Visual representation of the binary gain $G_{TR}(i,j)$ for a transmitting node i and a receiving node j.

By assuming for simplicity that all primary antennas have a unitary gain, $I_R(i,p)$ $\forall i,p$ is thus defined as:

$$I_R(i,p)=P_T(i)G_T(i)G_\alpha(i,p)G_{TP}(i,p). \quad (9)$$

Because of power attenuation as a function of distance, from a transmitting node, the received power might be so small at a receiving node or primary antenna that it becomes irrelevant, even as interference, so we consider it to be null. Hence, we define the minimal non zero power P_{MNZ} as the power threshold from which any lower power is automatically set to null. When a transmitting node i uses the transmission power $P_T(i)$, we consider the distance from i's location, at which the power reaches P_{MNZ}, by neglecting the slow fading for such a small power and setting $C(i,j) = 1$, to be $r_{MNZ}(i)$ and defined as:

$$r_{MNZ}(i)=\sqrt[\alpha]{\frac{P_T(i)G_T(i)}{P_{MNZ}}}, \quad (10)$$

which is obtained from (7) with replacements: $P_R(i,j) \rightarrow P_{MNZ}$, $G_\alpha(i,j) \rightarrow r_{MNZ}(i)^{-\alpha}C(i,j)$, $G_R(j) \rightarrow 1$ and $G_{TR}(i,j) \rightarrow 1$.

B. Communication and interference model

We use roughly the same interference model as in [13] for the MANET. Let γ_{SINR} be the SINR threshold for which a communication link with transmitting node i is considered successful toward a receiving node j, in the presence of other interfering transmitted power from $\forall h\in S_T | h\neq i$. The chosen constant noise power N_R, at the listening nodes, takes into account the interference generated by the primary antennas to the MANET, in addition to the thermal noise. The condition for such a link to be successful is then:

$$\frac{P_R(i,j)}{N_R G_R(j)+\sum_{\forall h\in S_T | h\neq i} P_R(h,j)}\ge\gamma_{SINR}, \quad (11)$$

the link is said to be failed otherwise.

A receiving node j is said to be in communication range of a transmitting node i if, by supposing there is no interference caused by any other transmitting node, it has its SNR $\ge \gamma_{SINR}$. The distance from i's location of this communication range to j's location is considered to be $r_{COM}(i,j)$. Let $r_{COM,e}(i)$ be the MANET estimate of $r_{COM}(i,j)$ which does not take the slow fading into account by setting $C(i,j) = 1$, so that it does not depend on j. $r_{COM}(i,j)$ and $r_{COM,e}(i)$ are defined as:

$$\left\{\begin{array}{c} r_{COM}(i,j)=\sqrt[\alpha]{\frac{P_T(i)G_T(i)C(i,j)}{\gamma_{SINR}N_R}}, \\ r_{COM,e}(i)=\sqrt[\alpha]{\frac{P_T(i)G_T(i)}{\gamma_{SINR}N_R}} \end{array}\right\}, \quad (12)$$

which are obtained from (7) with replacements: $P_R(i,j) \rightarrow \gamma_{SINR}N_R G_R(j)$, $G_\alpha(i,j) \rightarrow r_{COM}(i,j)^{-\alpha}C(i,j)$ and $G_{TR}(i,j) \rightarrow 1$.

IV. PROPOSED INTERFERENCE ESTIMATION TECHNIQUE

From what has been discussed in section II, we now show how the MANET can use Ω_{UC} as a way to adequately overestimate the aggregate interference it causes to the primary antennas.

We define $r_{INT}(i,p)$ as the interference radius from a transmitting node i to a primary p, which would result on $I_R(i,p)$. If $I_R(i,p) = 0$ then $r_{INT}(i,p)$ is not considered and can have any arbitrary value, otherwise $r_{INT}(i,p) = d(i,p)$. The MANET estimate of $r_{INT}(i,p)$ is $r_{INT,e}(i,p)$ so that if $I_{R,e}(i,p) = 0$ then $r_{INT,e}(i,p)$ is also not considered, otherwise $r_{INT,e}(i,p)$ is a bit more tricky to obtain as explained in the following.

The MANET considers that node i causes interference to primary p if its transmission sector overlaps p's UC. Indeed, if i lies outside p's UC, the MANET considers the interference that i causes to the closest point on p's UC edge for the value of $I_{R,e}(i,p)$. On the other hand, if i lies inside p's UC, the MANET considers the interference that i causes to the same point as i's own location for the value of $I_{R,e}(i,p)$.

If i lies outside p's UC, let $\beta(i,p)$ be the angle formed by two lines tangent to the UC, on opposite sides of it, and joining at i, as shown on Fig. 2, and let $\Delta_{T,e}(i,p)$ be the MANET estimate of $\Delta_T(i,p)$.

Let $G_{TP,e}(i,p)$ be the MANET estimate of $G_{TP}(i,p)$, then:

$$G_{TP,e}(i,p) = \begin{cases} r_{INT,e}(i,p)^{\alpha}, & \text{if } \left(d_e(i,p) \le R_{UC}(p)\right) \\ 1, & \text{if } \left\{ \begin{array}{l} \left(d_e(i,p) > R_{UC}(p)\right) \wedge \\ \left(\Delta_{T,e}(i,p) < \left(\frac{\theta(i)+\beta(i,p)}{2}\right)\right) \end{array} \right\} \\ 0, & \text{otherwise} \end{cases} . \quad (13)$$

$I_{R,e}(i,p)$ is thus defined as:

$$I_{R,e}(i,p) = P_T(i) G_T(i) r_{INT,e}(i,p)^{-\alpha} G_{TP,e}(i,p), \quad (14)$$

which is obtained from (9) with replacements: $I_R(i,p) \rightarrow I_{R,e}(i,p)$, $G_a(i,p) \rightarrow r_{INT,e}(i,p)^{-a} C(i,p)$, $C(i,p) \rightarrow 1$ and $G_{TP}(i,p) \rightarrow G_{TP,e}(i,p)$.

Note that the gain $G_{TP,e}(i,p)$ is not binary like its counterpart $G_{TP}(i,p)$. Indeed, the reason for having the first possible value of $G_{TP,e}(i,p)$ in (13) is to cancel the path loss effect in (14), in the special case where i lies inside p's UC. If $G_{TP,e}(i,p) = 0$ then $r_{INT,e}(i,p)$ is not considered, and if $G_{TP,e}(i,p) = r_{INT,e}(i,p)^{\alpha}$ then $r_{INT,e}(i,p)$ is cancelled in (14). The remainder of this section demonstrates how to find $r_{INT,e}(i,p)$ in the case where $G_{TP,e}(i,p) = 1$.

When i lies outside p's UC, two cases may occur giving $G_{TP,e}(i,p) = 1$, depending on the value of $\Delta_{T,e}(i,p)$, which influences the way we calculate $r_{INT,e}(i,p)$. The first case occurs if $0 \le \Delta_{T,e}(i,p) \le \theta(i)/2$, for which we have to find the value of $r_{INT,e}(i,p)$ such that the resulting arc on i's sector is tangent to p's UC. Then we simply have $r_{INT,e}(i,p) = d_e(i,p) - R_{UC}(p)$.

The second case occurs if

$$\Delta_{T,e}(i,p) \in \left]\frac{\theta(i)}{2}, \left(\frac{\theta(i)}{2} + \frac{\beta(i,p)}{2}\right)\right[, \quad (15)$$

for which the grey triangle formed on Fig. 3 can be used to find the value of $r_{INT,e}(i,p)$.

We assign the grey triangle sides on Fig. 3 to $a = r_{INT,e}(i,p)$, $b = d_e(i,p)$, $c = R_{UC}(p)$, and also the already known angle $\omega_C = \Delta_{T,e}(i,p) - \theta(i)/2$. Hence, we get the order 2 polynomial as a function of a, from the law of cosines:

$$a^2 - 2b\cos(\omega_C)a + (b^2 - c^2) = 0, \quad (16)$$

with roots given by:

$$a = b\cos(\omega_C) \pm \sqrt{b^2(\cos^2(\omega_C) - 1) + c^2}. \quad (17)$$

The smallest root of this polynomial gives the length of a intersecting with p's UC without passing through it yet, while the greatest root gives the length of a passing through the circle before intersecting with it for the second time. Thus, we are only interested in the first root, and $r_{INT,e}(i,p)$ is given by:

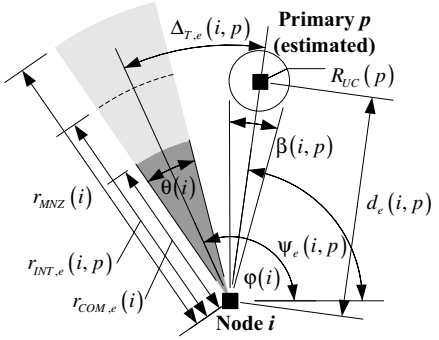

Figure 2. Visual representation of the variables defining the relation between a transmitting node i and a primary antenna p (with $r_{INT,e}(i,p)$ having an arbitrary value).

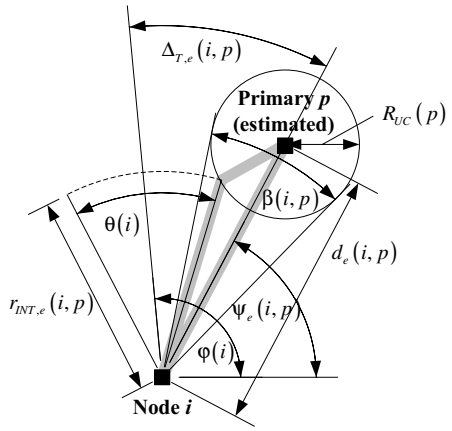

Figure 3. Visual representation of the second case in calculating $r_{INT,e}(i,p)$ when $G_{TP,e}(i,p) = 1$.

$$r_{INT,e}(i,p) = d_e(i,p)\cos\left(\Delta_{T,e}(i,p) - \frac{\theta(i)}{2}\right) - \sqrt{\frac{\cos^2\left(\Delta_{T,e}(i,p) - \frac{\theta(i)}{2}\right) - 1}{d_e(i,p)^{-2}} + R_{UC}(p)^2}. \quad (18)$$

Once $r_{LIM,e}(i,p)$ is known, $I_{A,e}(p)$ can be calculated from (2) and (14). Finally, $I_{A,o}(p)$ $\forall p \in S_P$ are easily calculated from (3) and the next section shows how to use our scheme by simulations.

V. Simulations

We performed 3 Monte Carlo simulations, each consisting of 10000 independent trials, to obtain empirical results with identical transmitting nodes beam width of $\theta(i) = \{60°, 120°, 360°\}$ $\forall i \in S_T$, the third one representing the use of omnidirectional antennas instead of smart antennas. However, the identical receiving nodes beam width of $\theta(j) = 60°$ $\forall j \in S_R$ remains the same for all 3 simulations. The reason behind this nodes beam width setting is to better asses the advantage of using smart antennas as a way to reduce the interference caused to a primary network, while always ensuring a relatively high connectivity among nodes by choosing a narrow reception beam width of 60°.

A. Procedure and input parameters

For each simulation trial, the MANET nodes are randomly placed in a 2D simulation area following a uniform distribution. In the same area, the estimated locations of the primary antennas, i.e. $(\mu_x(p),\mu_y(p))$ $\forall p \in S_P$, are also placed following a uniform distribution. Then, a bivariate Gaussian distribution is used to randomly place the actual locations of the primary antennas, i.e. $(x(p),y(p))$, with means $(\mu_x(p),\mu_y(p))$ and standard deviations $\sigma_{xy}(p)$ on both axes, for all $p \in S_P$, where all $\sigma_{xy}(p)$ are randomly set from a uniform distribution. These actual primary antennas locations, i.e. $(x(p),y(p))$ $\forall p \in S_P$, may lie outside the simulation area but still be considered.

After the location setup is done, communication links have to be established among MANET nodes in order to simulate the interference they cause to the primary antennas. Each node has its antenna beam steered directly toward its peer if it forms a link, otherwise no beam is used as such a node is thus considered idle. Appendix A presents the algorithm we have created to ensure a relatively high MANET connectivity composed of only successful links. We call this algorithm: CSRRT (*Closest Successful Receiver to Random Transmitters*) and the results depend on the chosen link factor ξ. This algorithm is clearly suboptimal, but easy to simulate while giving a rather realistic connectivity. Although failed links are unfortunately abundant in real world communications, there is no need to consider them as they do not affect our simulation results in any way.

It has to be noted that the MANET nodes and primary antenna locations (actual as well as estimated for the latter) are generated once, thus 10000 different scenarios only. These same scenarios are then used for the 3 transmitting nodes beam width settings. This gives a total of 30000 MANET connectivities. For each such MANET connectivity, $I_{A,o}(p)$ $\forall p \in S_P$ are calculated for $\Omega_{UC} = \{0.0, 1.0, 2.0, \ldots, 80.0\}$, hence 81 times. In other words, $I_{A,o}(p)$ $\forall p \in S_P$ are thus calculated for a total of 2430000 times, which are however analyzed separately in 3 groups. Table I summarizes all identical input parameters used for each simulation trial.

B. Results and interpretation

The simulation results are presented in Fig. 4, representing $P(I_{A,o}(p) > I_{A,SM})$ $\forall p \in S_P$, but it is actually $P(I_{A,o}(p) \leq I_{A,SM})$ $\forall p \in S_P$ which is displayed, as it is more appropriate for further explanation, and the former is simply the complement of the latter. Fig. 4 (a) and (b) present the results for $\theta(i) = 60°$ $\forall i \in S_T$, (c) and (d) for $\theta(i) = 120°$ $\forall i \in S_T$, and (e) and (f) for $\theta(i) = 360°$ $\forall i \in S_T$. As can be seen, the left hand side of Fig. 4 presents the results as a function of Ω_{UC} with curves for different values of $I_{A,SM}$, while the right hand side presents the results as a function of $I_{A,SM}$ with curves for different values of Ω_{UC}. Also included in Fig. 4 are two meaningful examples:

1. The primary network imposes the requirement (4) to the MANET with $I_{A,SM} = 2.0$ watts and $\eta_{SM} = 0.7$, marked by the dashed lines on the left hand side and equivalently the dotted lines on the right hand side of Fig. 4, respectively.
2. The MANET assesses the limit requirement (4) that it could accept from the primary network while still working properly (i.e. worst case), specifically with a maximal value of $\Omega_{UC} = 40.0$ with a cautious probability of $\eta_{SM} = 0.8$, marked by the dashed lines on the right hand side and equivalently the dotted lines on the left hand side of Fig. 4, respectively.

For the first example, we observe that by increasing the transmitting nodes beam width, the MANET has to increase Ω_{UC} in order to respect the primary network requirement. By using omnidirectional antennas, it becomes even impossible to respect the requirement as a limit is reached at about $\eta_{SM} = 0.68$ for $I_{A,SM} = 2.0$ watts, so that even increasing Ω_{UC} to more than 80.0 would be completely useless. Based on Fig. 4 (a) and (b), the MANET can choose to whether set the beams width to

TABLE I
SIMULATION TRIAL INPUT PARAMETERS

MANET and Primaries	Communication
Simulation area = 1 km × 1 km	$N_R = 10^{-7}$ mw
$\theta(j) = 60°$, $\forall j \in S_R$	$\gamma_{SINR} = 63.0$ (18 dB)
Number of nodes = 30	$P_{MNZ} = 10^{-8}$ mw
Number of primary antennas = 7	$d_0 = 1.0$ m
$\sigma_{xy}(p) \sim$ U[10, 30] m, $\forall p \in S_P$	$\alpha = 2.1$
$\xi = 1.2$	$\sigma_C = 0.2$

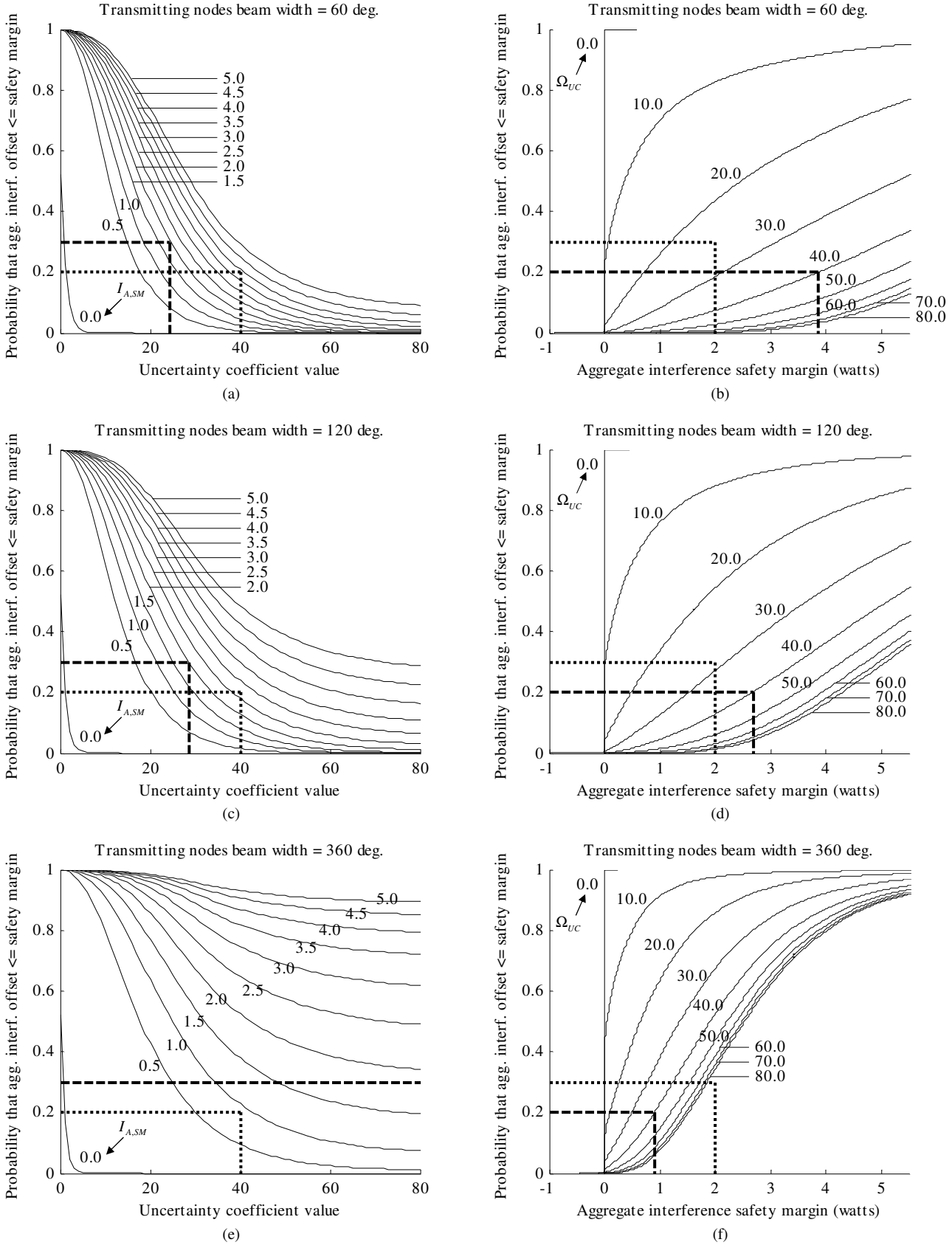

Figure 4. Empirical results of $P(I_{A,o}(p) \leq I_{A,SM}) \; \forall p \in S_P$ for Ω_{UC} from 0.0 to 80.0 and $I_{A,SM}$ from 0.0 to 5.0 watts: (a) curves of $I_{A,SM}$ as a function of Ω_{UC} with $\theta(i) = 60° \; \forall i \in S_T$, (b) curves of Ω_{UC} as a function of $I_{A,SM}$ with $\theta(i) = 60° \; \forall i \in S_T$, (c) curves of $I_{A,SM}$ as a function of Ω_{UC} with $\theta(i) = 120° \; \forall i \in S_T$, (d) curves of Ω_{UC} as a function of $I_{A,SM}$ with $\theta(i) = 120° \; \forall i \in S_T$, (e) curves of $I_{A,SM}$ as a function of Ω_{UC} with $\theta(i) = 360° \; \forall i \in S_T$, (f) curves of Ω_{UC} as a function of $I_{A,SM}$ with $\theta(i) = 360° \; \forall i \in S_T$.

60° or 120° upon its deployment, as long as it also sets $\Omega_{UC} = 22.3$ or $\Omega_{UC} = 24.2$, respectively.

For the second example, still by increasing the transmitting nodes beam width of the MANET, the possibilities of being accepted by the primary network to share the same spectrum decrease, as this would assume a decrease in the value of $I_{A,SM}$ from requirement (4) with $\eta_{SM} = 0.8$. The requirement of the second example is more attractive for the primary network than that of the first one when the beams width is set to 60° or 120°. However, with the use of omnidirectional antennas, the requirement of the second example is less attractive, but is realizable as opposed to the first example requirement.

From the primary network point of view, the larger is the Ω_{UC} value used by the MANET, the larger would be the $I_{A,o}(p)$ $\forall p \in S_P$, so a large Ω_{UC} is always desirable. From the MANET point of view however, having large $I_{A,o}(p)$ $\forall p \in S_P$ values means a large overestimation of the interference caused to the primary network by the MANET, so a smaller value of Ω_{UC} is always preferred.

C. Discussion

On the right hand side of Fig. 4, one can see that $I_{A,o}(p)$ $\forall p \in S_P$ practically does not exceed the range of [-1.0, 1.0] watts for $\Omega_{UC} = 0.0$ during all simulation trials. In fact, this range is mainly related to the limits of the uniform distribution used to set $\sigma_{xy}(p)$ $\forall p \in S_P$, and clearly shows the importance of using an UC if the requirement (4) is to be considered by the MANET. Also, without an UC, the difference between the actual and estimated aggregate interferences cannot be very high when using as many as 30 nodes, since individual interference overestimation and underestimation may partly cancel each other if σ_C is reasonably low. In addition, these curves for $\Omega_{UC} = 0.0$ are very steep because most values of $I_{A,o}(p)$ $\forall p \in S_P$ are very close to zero either on positive or negative side and only few minority gets visibly distant from zero. There is still a very few negative values with the curves for $\Omega_{UC} = 10.0$ on Fig 4. (b), (d) and (f) but they are all positive for $\Omega_{UC} = 20.0$ and above.

The steepness of the curve for any value of Ω_{UC}, still on the right hand side of Fig. 4, could also be a good criterion to consider when evaluating the interference the MANET could cause to the primary network. For instance with beams width of 60°, the low curve steepness for $\Omega_{UC} = 40.0$ gives a kind of insurance for the primary network that not only is the requirement (4) respected, but also that $P(I_{A,o}(p) \leq I_{A,SM})$ $\forall p \in S_P$ is not as likely to occur as for with beams width of 360°, for the high curve steepness of the latter.

On the left hand side of Fig. 4, there is a remarkable distance between the curves for $I_{A,SM} = 0.0$ and 0.5 watts. At the very beginning of the abscissa, i.e. at $\Omega_{UC} = 0.0$, one can see that the curves for $I_{A,SM} = 0.0$ watts have a value of about 0.5 on the ordinate. This can be interpreted directly with the help of the curves for $\Omega_{UC} = 0.0$ on the right hand side. Indeed, about half the points composing these curves are for negative values of $I_{A,o}(p)$ $\forall p \in S_P$. The aforementioned distance thus comes from the fact that even for a very small value of $I_{A,SM}$ greater than zero, $P(I_{A,o}(p) \leq I_{A,SM})$ $\forall p \in S_P$ gets very close to 1.0. The limit clearly shown in Fig. 4 (e) and (f), for $I_{A,SM} = 2.0$ watts and $\eta_{SM} = 0.7$, is directly related to the dimension of the simulation area, as compared to the UC of each primary antenna. Indeed, if a given UC is too large, it will cover more than the simulation area and the actual location of the antenna will also be very likely to lie inside the UC. Thus, further increasing Ω_{UC} would not increase η_{SM} significantly. Because of P_{MNZ} in our propagation model, if the bivariate Gaussian distribution puts the actual location of a primary antenna too far from its estimated location (such a distribution could theoretically yield an infinite distance between both locations), its actual aggregate interference would be null. That is the reason why even with an infinite number of simulation trials and an infinite computer precision, the limit will be reached, hence it is not an asymptote and is also more realistic.

The curves presented in Fig. 4 could have a very different scale by changing any of the simulation parameters. Augmenting the number of nodes or number of primary antennas increases exponentially the required simulation time. Most importantly, one should be aware that these results strongly depend on our antenna and propagation model as well as our CSRRT algorithm to generate communication links among MANET nodes. While using more precise models could be preferable, we can say without lose of generality that the resulting simulation curves for $I_{A,SM}$ and Ω_{UC} would follow the same trend as presented on Fig. 4, but with a different scale, added to the fact that the MANET could take even better decisions.

VI. Conclusion

An interference safety margin approach has been addressed in this paper to prevent a MANET (secondary wireless network) from strongly interfering with a primary wireless network composed of fixed antennas. This can be realized by forcing the MANET to overestimate the aggregate interference it causes to each primary antenna. With the help of our proposed interference estimation technique, the MANET can probabilistically decide the magnitude of its overestimation, so as to respect the requirement imposed by the primary network, following a given safety margin probability.

Our work's originality resides in the fact that the MANET only knows the probabilistic location of each primary antenna. Indeed, the possibly very poor interaction between both networks solely allows the MANET to have a coarse estimate of each primary antenna location. Furthermore, our scheme is especially designed to take advantage of the smart antenna technology, for which cognitive radio devices are very likely to be equipped in the near future.

Sustained by our simulation results, our scheme has been proven to be very useful prior any cognitive radio system deployment.

APPENDIX A THE CSRRT ALGORITHM

This appendix describes our CSRRT algorithm we use to generate a relatively high number of successful one-hop communication links between MANET nodes (see section III.B). A link is composed of only one transmitting/receiving nodes pair, respectively denoted as nodes i and j. For convenience, we ensure that each link's SNR equals $\gamma_{SINR}\xi$, where ξ is a chosen link factor (the interference is not considered to be part of the noise), so i's transmission power is set to:

$$P_T(i) = \frac{\gamma_{SINR}\xi N_R}{G_T(i)G_\alpha(i,j)}, \quad (19)$$

which is obtained from (7) with replacements: $P_R(i,j) \rightarrow \gamma_{SINR}\xi N_R G_R(j)$ and $G_{TR}(i,j) \rightarrow 1$.

We define a link as "accepted" if two rules are simultaneously satisfied (the link being "rejected" otherwise):

1. The link must be successful despite the presence of all other accepted links;
2. All accepted links must remain successful despite the acceptance of this link.

The algorithm is presented on Fig. 5. The objective is to fill the matrix M_{Links} with as much successful links as possible (no failed links).

ACKNOWLEDGMENT

The authors wish to thank Professor André Girard for his precious help in establishing the right antenna, interference and communication models.

```
N_Nodes = Number of MANET nodes
V_Nodes = Radom permutation of [1, 2, …, N_Nodes] //Unique ids
M_Links = [] //Empty matrix of all MANET links, dimension 0×2
V_Not_TX = []
for i = V_Nodes
   if (i ~= V_Nodes(end))
      V_Temporary = V_Nodes((i+1):end)∪V_Not_TX
   else
      V_Temporary = V_Not_TX
   end
   V_Temporary = Ascending ordering of V_Temporary w.r.t. i
                 // i is the transmitter, and all elements of V_Temporary
                 // are potential receivers (only one chosen), they
                 // are thus ordered with respect to their respective
                 // physical distance to i. The remainder of the
                 // algorithm tries to choose the closest node as the
                 // receiver (if the link is successful).
   flag_successful = false;
   for j = V_Temporary
      if (i and j forms a successful link)
         M_Links(end+1, :) = [i, j]
         flag_successful = true
         break
      end
   end
   if (~flag_successful)
      V_Not_TX(end+1) = i
   end
end
```

Figure 5. Our CSRRT algorithm to generate a relatively high number of successful MANET links, based on *Matlab* scripting language.

REFERENCES

[1] FCC, "Spectrum policy task force report. et docket no. 02-135," November 2002.
[2] J. Yang, "Spatial channel characterization for cognitive radios," MS Thesis, UC Berkeley, 2004.
[3] Senhua Huang, Zhi Ding, and Xin Liu, "Non-Intrusive Cognitive Radio Networks based on Smart Antenna Technology," *IEEE Global Telecommunications Conference (GLOBECOM)*, pp. 4862-4867, November 2007.
[4] D. Cabric, S.M. Mishra, D. Willkomm, R.W. Brodersen, A. Wolisz, "A Cognitive Radio Approach for Usage of Virtual Unlicensed Spectrum," *IST Mobile and Wireless Communications Summit, 14th*, June 2005.
[5] P. Hoven and A. Sahai, "Power Scaling for Cognitive Radio," *International Conference on Wireless Networks, Communications and Mobile Computing, IEEE*, vol. 1, pp. 250-255, 13-16 June 2005.
[6] B. Wild and K. Ramchandran, "Detecting Primary Receivers for Cognitive Radio Applications," *IEEE 1st International Symposium on New Frontiers in Dynamic Spectrum Access Networks*, pp. 124-130, Baltimore, MD, USA, November 2005.
[7] S. M. Mishra, R. Tandra, and A. Sahai, "Coexistence with primary users of different scales," *IEEE 2nd International Symposium on New Frontiers in Dynamic Spectrum Access Networks*, pp. 158-167, Dublin, Ireland, April 2007.
[8] J.K. Nelson, M.U. Hazen, and M.R. Gupta, "Global Optimization for Multiple Transmitter Localization," *Military Communications Conference (MILCOM'06), IEEE*, pp. 1-7, October 2006.
[9] J.K. Nelson and M.R. Gupta, "An EM Technique for Multiple Transmitter Localization," *41st Annual Conference on Information Sciences and Systems (CISS'07), IEEE*, pp. 610-615, March 2007.
[10] P. Kontkanen, P. Myllymäki, T. Roos, H. Terri, K. Valtonen, and H. Wettig, "Topics in Probabilistic Location Estimation in Wireless Networks," *15th IEEE International Symposium on Personal, Indoor and Mobile Radio Communications (PIMRC'04)*, vol. 2, pp. 1052-1056, Barcelona, Spain, September 2004.
[11] M. Boutin, A. Benzakour, C. L. Despins, and S. Affes, "Radio Wave Characterization and Modeling in Underground Mine Tunnels," *IEEE Transactions on Antennas and Propagation*, vol. 56, no. 2, pp. 540-549, February 2008.
[12] S. Vasudevan, J. Kurose, and D. Towsley, "On Neighbor Discovery in Wireless Networks with Directional Antennas," *INFOCOM 2005, 24th Annual Joint Conference of the IEEE Computer and Communications Societies. Proceedings IEEE*, vol. 4, pp. 2502-2512, March 2005.
[13] P. Björklund, P. Värbrand, and D. Yuan, "Resource Optimization of Spatial TDMA in Ad Hoc Radio Networks: A Column Generation Approach," *INFOCOM 2003, 22th Annual Joint Conference of the IEEE Computer and Communications Societies, IEEE*, vol. 2, pp. 818-824, April 2003.

Mathieu Boutin received the Bachelor's degree in computer science engineering from the École Polytechnique de Montréal, Montreal, QC, Canada, in 2002, and the Master's degree from INRS-EMT, Université du Québec, Montreal, in 2005, where he is currently working toward the Ph.D. degree.

His research interests are in radio wave propagation and cognitive wireless *ad hoc* networks.

Charles Despins (**S'84–M'94–SM'02)** holds a bachelor's degree in electrical engineering from McGill University in Montreal, Canada as well as M.Sc. and Ph.D. degrees, also in electrical engineering, from Carleton University in Ottawa, Canada.

In addition to his work as a faculty member of INRS-Telecommunications (Université du Québec) in Montreal, Canada, he has held senior posts in the private sector, namely at Microcell Telecom inc. (Canadian GSM operator) and at Bell Nordiq Group (a network operator in rural and northern areas of Canada) as vice-president and chief technology officer. He has also worked as a consultant for various wireless network deployments in India and China. Since January 2003, he has been president and CEO of Prompt inc., an ICT university-industry research and development consortium. He also remains active in university research as an adjunct professor at Université du Québec with research interests in wireless communications and networks. Dr. Despins is a Fellow of the Engineering Institute of Canada and received in 2006, the Outstanding Engineer award from IEEE Canada. He is a member of various company Boards including iBWave Solutions inc., the National Bank of Canada's startup of the year in 2007.

Tayeb A. Denidni (M'98-SM'04) received the B.Sc. degree in electronic engineering from the University of Setif, Setif, Algeria, in 1986, and the M. Sc. and Ph.D. degrees in electrical engineering from Laval University, Quebec City, QC, Canada, in 1990 and 1994, respectively.

From 1994 to 1996, he was an Assistant Professor with the engineering department, Université du Quebec in Rimouski (UQAR), Quebec, Canada. From 1996 to 2000, he was also an Associate Professor at UQAR, where he founded the Telecommunications laboratory. Since August 2000, he has been with the Personal Communications Staff, Institut National de la Recherche Scientifique (INRS-EMT), Université du Québec, Montreal, Canada. He founded the RF laboratory, INRS-EMT, Montreal, for graduate student research in the design, fabrication, and measurement of antennas. He has 10 years of experience with antennas and microwave systems and is leading a large research group consisting of two research scientists, five Ph.D. students, and three M.S. students. Over the past ten years he has graduated many graduated students. He served as the Principal Investigator on many research projects on antennas for wireless communications.

His current research interests include planar microstrip filters, dielectric resonator antennas, EBG antennas, antenna arrays, microwave and RF design for wireless applications. Dr. Denidni is a Member of the Order of Engineers of the Province of Quebec, Canada. He is also a Member of URSI (Commission C). He has authored more than 50 papers in refereed journals. He has also had more than 100 papers and invited presentations in numerous national and international conferences and symposia.

Sofiène Affes (**S'94–M'95–SM'04**) received the Diplôme d'Ingénieur in electrical engineering and the Ph.D. degree (with honors) in signal processing both from the École Nationale Supérieure des Télécommunications (ENST), Paris, France, in 1992 and 1995, respectively.

In 1995, he joined the INRS-EMT, University of Quebec, Montreal, QC, Canada, where he was a Research Associate from 1995 to 1997, an Assistant Professor from 1997 to 2000, and he is currently an Associate Professor in the Wireless Communications Group. His research interests are in wireless communications, statistical signal and array processing, adaptive space-time processing and MIMO. From 1998 to 2002, he led the radio-design and signal processing activities of the Bell/Nortel/NSERC Industrial Research Chair in Personal Communications at INRS-EMT. Currently he is actively involved in a major project in wireless of PROMPT-Quebec (Partnerships for Research on Microelectronics, Photonics and Telecommunications).

Prof. Affes is the co-recipient of the 2002 Prize for Research Excellence of INRS and currently holds a Canada Research Chair in Wireless Communications. He served as a General Co-Chair of the IEEE VTC'2006-Fall conference, Montreal, Canada, and currently acts as a member of Editorial Board of the Wiley Journal on Wireless Communications and Mobile Computing.